Article

Current Biology

Involvement of A13 dopaminergic neurons in prehensile movements but not reward in the rat

Highlights

- A13 dopamine cell activity relates to prehensile actions
- A reduction in A13 activity leads to deficits in grasping and handling of objects
- Movement-related A13 dopamine activity is unrelated to reward or reward consumption
- A13 dopamine neurons innervate the superior colliculus and reticular formation

Authors

Celia Garau, Jessica Hayes, Giulia Chiacchierini, James E. McCutcheon, John Apergis-Schoute

Correspondence

celiagarau@gmail.com (C.G.), j.apergis-schoute@qmul.ac.uk (J.A.-S.)

In brief

Garau et al. show that A13 dopamine neurons are important for movements linked to prehensile actions, but their activity is unrelated to reward. A13 neurons project to the superior colliculus and reticular formation—regions important for reach-to-grasp actions—positioning A13 within circuits that control handling and grasping.

Garau et al., 2023, Current Biology *33*, 4786–4797
November 20, 2023
https://doi.org/10.1016/j.cub.2023.09.044

CellPress

CellPress
OPEN ACCESS

Current Biology

Article

Involvement of A13 dopaminergic neurons in prehensile movements but not reward in the rat

Celia Garau,[1,*] Jessica Hayes,[1] Giulia Chiacchierini,[1,2,3] James E. McCutcheon,[1,4] and John Apergis-Schoute[1,5,6,*]
[1]Department of Neuroscience, Psychology & Behaviour, University of Leicester, University Road, Leicester LE1 9HN, UK
[2]Department of Physiology and Pharmacology, La Sapienza University of Rome, 00185 Rome, Italy
[3]Laboratory of Neuropsychopharmacology, Santa Lucia Foundation, 00143 Rome, Italy
[4]Department of Psychology, UiT The Arctic University of Norway, Huginbakken 32, 9037 Tromsø, Norway
[5]Department of Biological and Experimental Psychology, Queen Mary University of London, London E1 4NS, UK
[6]Lead contact
*Correspondence: celiagarau@gmail.com (C.G.), j.apergis-schoute@qmul.ac.uk (J.A.-S.)
https://doi.org/10.1016/j.cub.2023.09.044

SUMMARY

Tyrosine hydroxylase (TH)-containing neurons of the dopamine (DA) cell group A13 are well positioned to impact known DA-related functions as their descending projections innervate target regions that regulate vigilance, sensory integration, and motor execution. Despite this connectivity, little is known regarding the functionality of A13-DA circuits. Using TH-specific loss-of-function methodology and techniques to monitor population activity in transgenic rats *in vivo*, we investigated the contribution of A13-DA neurons in reward and movement-related actions. Our work demonstrates a role for A13-DA neurons in grasping and handling of objects but not reward. A13-DA neurons responded strongly when animals grab and manipulate food items, whereas their inactivation or degeneration prevented animals from successfully doing so—a deficit partially attributed to a reduction in grip strength. By contrast, there was no relation between A13-DA activity and food-seeking behavior when animals were tested on a reward-based task that did not include a reaching/grasping response. Motivation for food was unaffected, as goal-directed behavior for food items was in general intact following A13 neuronal inactivation/degeneration. An anatomical investigation confirmed that A13-DA neurons project to the superior colliculus (SC) and also demonstrated a novel A13-DA projection to the reticular formation (RF). These results establish a functional role for A13-DA neurons in prehensile actions that are uncoupled from the motivational factors that contribute to the initiation of forelimb movements and help position A13-DA circuits into the functional framework regarding centrally located DA populations and their ability to coordinate movement.

INTRODUCTION

The activity of centrally located dopamine (DA) neurons is critically important in transforming intent into action.[1–6] Classified according to the cell group nomenclature A8 to A16,[7,8] spatially distinct DA cell populations have been linked to the reinforcing properties of salient stimuli[9–11] and motor control[12–15] that, when coupled, result in effort-based planning and execution that is critical for goal-directed behavior.[16–19] Although this framework is mostly supported by research investigating DA neurons residing in the A9 ventral tegmental area and A10 substantia nigra pars compacta, separate studies have demonstrated that other unique DA populations also contribute to motor and reward-based processes. For instance, activation of diencephalic A11-DA neurons in the posterior hypothalamus has been shown to modulate locomotor behavior, potentially via their projections to the spinal cord.[20] By contrast, A12-DA neurons located ventrally in the arcuate nucleus of the hypothalamus signal reward related to food—a functional consequence likely mediated through their excitatory and inhibitory influence onto hunger and satiety-signaling cell populations, respectively.[21]

Anatomical work investigating projection patterns of A13-DA neurons suggests that this DA population may also be important for motor planning and/or motivation. Located in the rostromedial division of the zona incerta, A13-DA neurons contain DA[22] and predominately send descending projections that innervate mesencephalic locomotor (MLR) regions linked to vigilance and locomotion[23] and to the superior colliculus (SC)[24] where sensory-motor integration coupled to fear-related defensive[25–27] and appetitive hunting/foraging behavior[28,29] occurs. Functional work on A13 subpopulations is, however, sparse, and as such, their contribution to such processes is unresolved. Our study aimed to investigate the functional properties of A13-DA neurons by focusing on their potential role in motivation and motor regulation. To do so, we used transgenic tyrosine hydroxylase (TH)-Cre rats for monitoring and manipulating A13-DA neuronal activity while animals were engaged in reward and motor-based behavioral tasks. Our results indicate that A13-DA neurons are critical for skilled forelimb movements (SFMs), specifically those involving prehensile actions, thereby revealing a novel DA system important for motor coordination and execution.

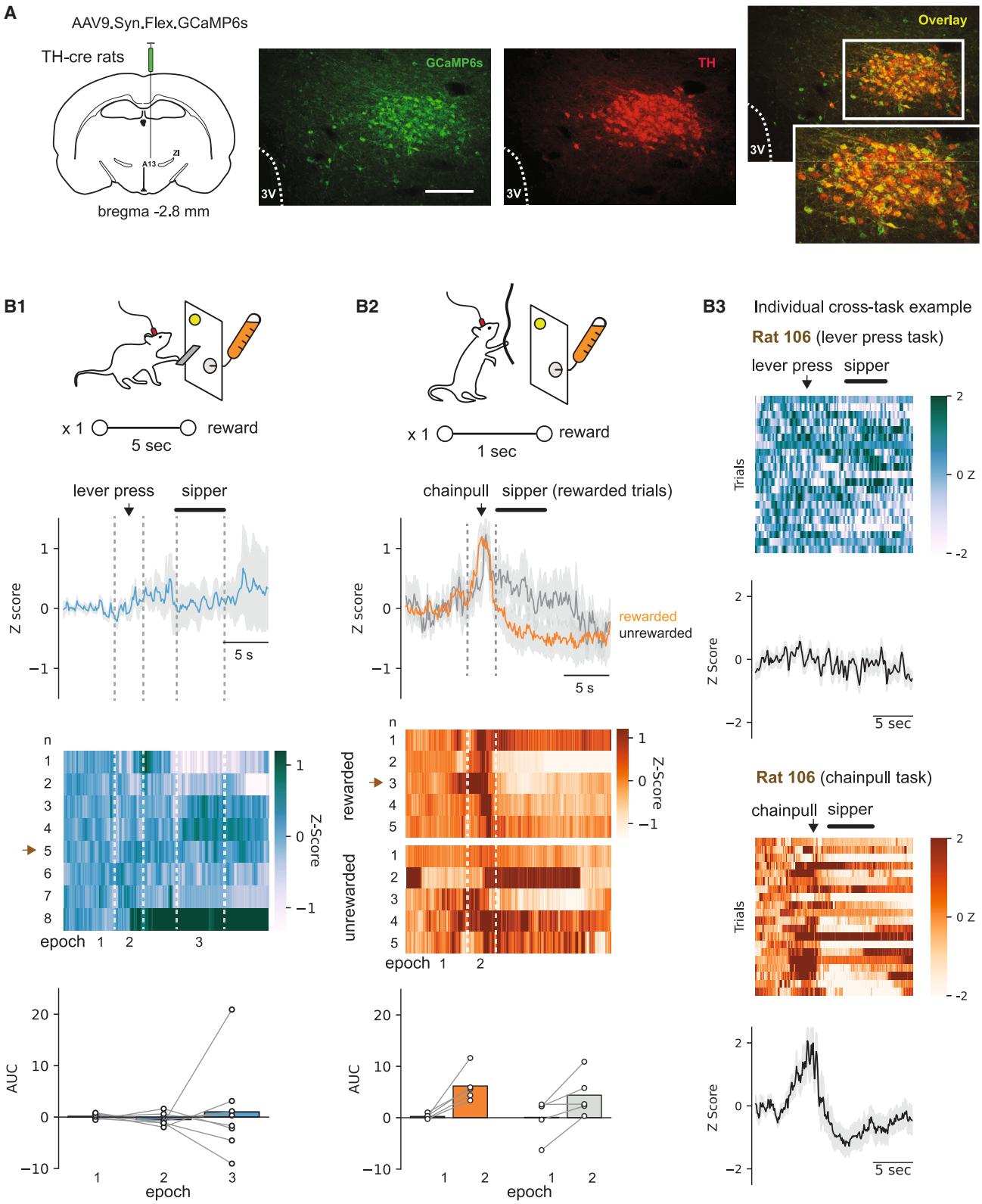

(legend on next page)

RESULTS

A13-DA neuronal activity relates to forelimb movements but not reward

To determine whether a relationship between A13-DA neuronal activity and motor and/or reward-based behavior exists, we monitored A13-DA activity using fiber photometry in TH-Cre rats with the Ca^{2+} indicator GCaMP6s expressed in A13-DA neurons (Figure 1A). Rats were trained to lever press (LP) and pull a chain (CP) (Figures 1B1 and 1B2, top) to access a sipper containing 10% sucrose solution on a fixed ratio (FR)1 schedule of reinforcement. For LP, a 5 s delay was imposed between the LP and sipper access, and for both tasks, a chamber light indicated the onset of an active trial where the lever was extended and a response would be reinforced. The chain was accessible between trials, allowing us to also analyze un-signaled and unrewarded CPs. We first measured LP fiber photometry signals during three epochs—baseline, in response to LP, and during sipper availability for LP—and a one-way repeated-measures (RM) ANOVA revealed no statistical difference between the signals ($F(2,14) = 0.133$, $p = 0.73$; $n = 8$; area under the curve [AUC]: baseline, 0.14 ± 0.17; LP, −0.47 ± 0.41; sipper, 1.00 ± 3.14) (Figure 1B1). By contrast, a two-way RM ANOVA for CP showed that both signaled/rewarded and un-signaled/unrewarded CP led to a significant increase in A13-DA activity compared with baseline, which did not differ by group (two-way RM ANOVA, epoch, $F(1,4) = 23.09$, $p = 0.01$; (un)rewarded, $F(1,4) = 0.44$, $p = 0.54$; interaction, $F(1,4) = 0.65$, $p = 0.47$; $n = 5$; AUC, baseline, rewarded/unrewarded, 0.25 ± 0.22/0.07 ± 1.68; CP, rewarded/unrewarded 6.17 ± 1.43/4.39 ± 1.85) (Figure 1B2). These responses were time-locked to the CP and unlikely triggered by cue onset since, on a trial-by-trial basis, the latency between cue onset and CP varied significantly (mean of all animals = 9.06 ± 1.46; Figure S1).

These findings demonstrate a link between A13-DA activity and forelimb responses. To further characterize A13-DA responses, we next tested whether A13-DA neurons respond to rewarding stimuli in an operant approach task that did not necessitate a specific forelimb action. To do so, we monitored A13-DA activity while animals were active in a two-bottle choice task where rats were given intermittent access to lick from two bottles, each containing a solution with different rewarding properties (Figure 2A). Since rats were given access to rewarding solutions without the need to LP, this task was used to gauge reward-based responses that were independent of forelimb movements. When given a choice between water and a 10% sucrose solution, rats licked the sucrose-containing sipper significantly more than the one containing water (paired t test: $p = 0.007$; total licks: water, 82.13 ± 22.77; sucrose, 631.63 ± 115.28, $n = 8$) (Figure 2A1, left bottom), thus showing a clear behavioral preference for the rewarding solution. When the corresponding photometry signals to licking of solution were analyzed, there were no significant changes in A13-DA activity compared with baseline when licking for sucrose (paired t test: $p = 0.83$; AUC: sucrose, baseline −0.02 ± 0.02; first lick, −0.44 ± 1.85; $n = 8$), but surprisingly, there was a significant increase to licking for water (paired t test: $p = 0.02$; AUC: water, baseline −0.02 ± 0.02; first lick, 4.15 ± 1.41; $n = 8$) (Figure 2A1, right). When water was replaced with a more palatable condensed milk (CM) solution (50% in water), there was similarly no change in activity for the sucrose solution (paired t test: $p = 0.72$; AUC: sucrose, baseline −0.003 ± 0.01; first lick −0.24 ± 0.64; $n = 8$) or, for that matter, the CM (paired t test: $p = 0.13$; CM, baseline, −0.03 ± 0.01; sipper, −2.25 ± 1.29; $n = 8$) (Figure 2A2, right) despite an increase in licking for CM that was comparable to that of sucrose (paired t test: $p = 0.52$; total licks: CM, 563.0 ± 46.00; sucrose, 599.86 ± 49.47; $n = 8$) (Figure 2A2, left bottom).

A13-DA activity is not causally related to LP or motivation for a reward

We next tested whether A13-DA activity directly influences forelimb movements and/or motivation toward a reward. For this, TH-Cre rats expressing designer receptors activated only by designer drugs (DREADDs) used for manipulating A13-DA activity were tested on LP behavioral tasks commonly used to investigate motivation.[30] Neuronal expression of Gq- and Gi-coupled DREADD receptors has been used to excite and inhibit neurochemically distinct neurons, respectively.[31] Expressing (Figure 2B1) and subsequently activating excitatory Gq-coupled or inhibitory Gi-coupled DREADDs on A13-DA neurons through intraperitoneal injections of the DREADD ligand clozapine N-oxide (CNO) had no impact on either an FR5 or progressive ratio (PR)5 LP task when compared with saline injections or to rats where only the reporter protein mCherry was expressed (FR5, two-way ANOVA, group, $F(2,36) = 0.95$, $p = 0.40$; saline/CNO, $F(1,36) = 0.06$, $p = 0.81$; interaction, $F(2,36) = 0.43$, $p = 0.66$) (Figure 2B2) (PR5, two-way ANOVA, group, $F(2,36) = 3.21$, $p = 0.05$; saline/CNO, $F(1,36) = 0.29$, $p = 0.60$; interaction, $F(2,36) = 0.75$, $p = 0.48$) (Figure 2B3) ($n = 7$ per each group). Overall, these results indicate that A13-DA activity is not required for reward-based motivation.

Fine forelimb movements are related to A13-DA activity and dependent on an intact A13-DA system

These results suggest that A13-DA neurons encode for prehensile actions and not for rewarding stimuli. In order to further test this idea, we trained TH-Cre rats on a skilled fine forelimb reaching and grasping task. Using a transparent Plexiglass chamber with a narrow opening at one end, rats learned to reach through the opening to access a sucrose pellet.[32] Following training, animals were able to successfully reach, grab, and consume over

Figure 1. A13-DA population activity relates to forelimb movements

(A) GCaMP6s-GFP expression in A13 immunocytochemically labeled (594 nm) TH-containing neurons of TH-Cre rats.

(B) A13-DA Ca^{2+} activity in response to the first LP following light onset for LP (B1) and CP to cue-signaled rewarded (orange trace) and un-signaled unrewarded trials (gray trace) (B2). Average photometry signal of LP onset and sipper availability (top) followed by color plot depicting the average of each rat (middle) and summary AUC data for baseline, LP, and sipper access (bottom). (B3) Response profile of an individual rat across LP and CP tasks. Brown arrows in (B1) and (B2) indicate rats depicted in cross-task individual trials (B3). Scale bars, 0.2 mm. 3V, 3rd ventricle.

Error bars represent the SEM. Related to Figure S1.

CellPress
OPEN ACCESS

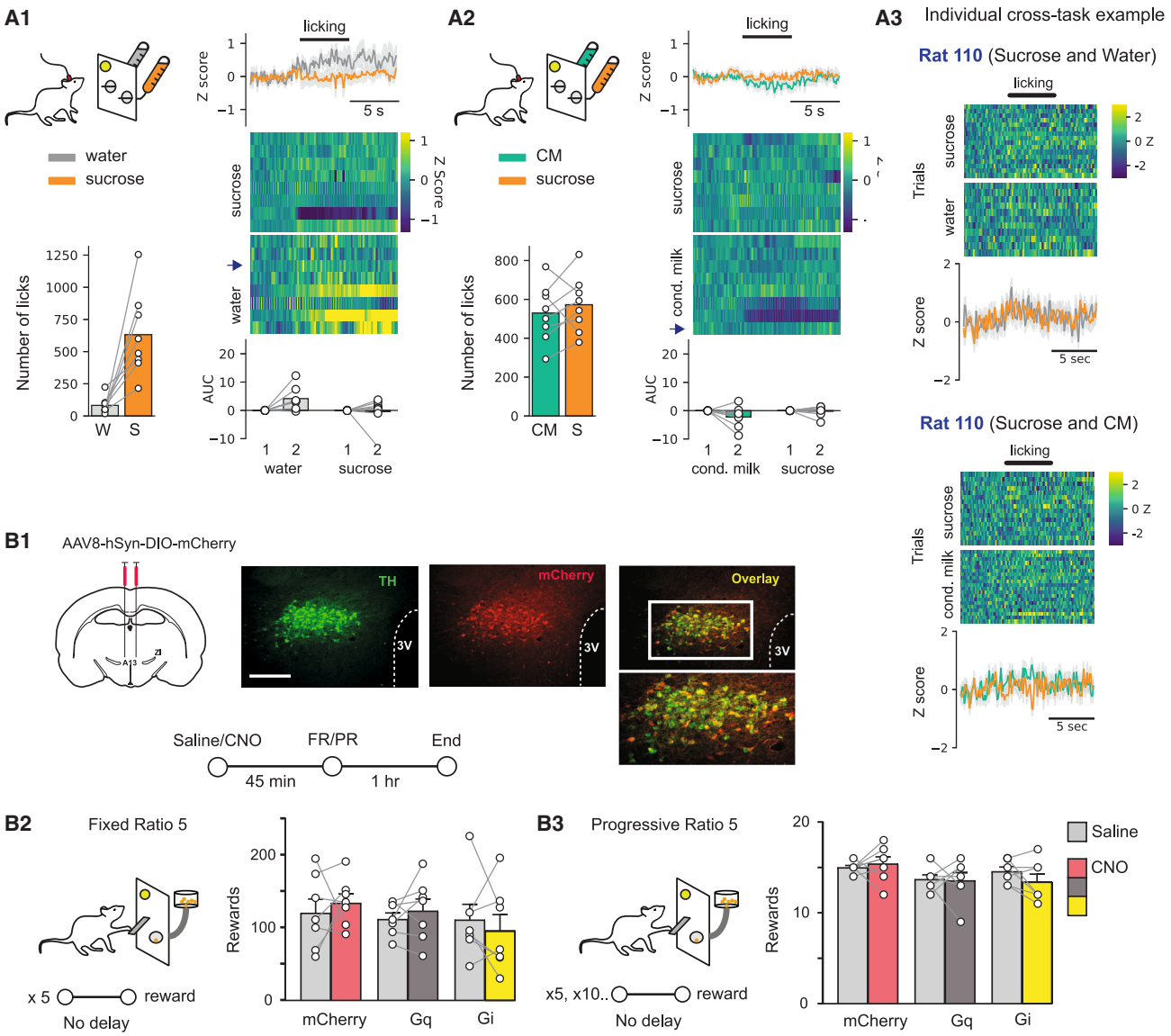

Figure 2. A13-DA activity is unrelated to motivated behavior toward reward delivery and consumption

(A) In a two-bottle preference test, A13 activity is unrelated to increases in licking for either a sucrose (A1) or a condensed milk (CM) (A2) solution. AUC analysis is aligned to the first lick following sipper extension. (A3) Response profile of an individual rat across sucrose/water and sucrose/CM tasks.

(B) A13-DA expression (B1) and manipulation of A13 activity did not affect motivation for a food reward on operant paradigms under FR5 (B2) or PR5 (B3) contingencies.

Error bars represent the SEM. Blue arrows in (A1) and (A2) indicate rats depicted in cross-task individual trials (A3). Scale bars, 0.2 mm (B1). 3V, 3rd ventricle; AUC, area under the curve; CNO, clozapine N-oxide; FR, fixed ratio; PR, progressive ratio.

80% of pellets during a session (50 trials/session). Relative to baseline, A13-DA activity significantly increased when rats successfully reached for and grasped sucrose pellets as well as when compared with unsuccessful reaching attempts (two-way RM ANOVA, epoch, $F(1,5) = 8.87$, $p = 0.03$; miss/success, $F(1,5) = 9.20$, $p = 0.03$; interaction, $F(1,5) = 9.63$, $p = 0.03$; $n = 6$; AUC: baseline, miss/success, $-0.41 \pm 0.45/-0.61 \pm 0.40$; reach, miss/success, $0.82 \pm 0.72/5.28 \pm 1.50$) (Figure 3A1), supporting a role for A13-DA neurons in grasping that is independent of forelimb reaching movements. Post-mortem analyses from 3 rats showed that of the 162 GCaMP6s-expressing neurons, 129 also contained TH (79.6%)—a proportion in line with previous results measuring cre expression in a TH-cre mouse line.[33]

To further shed light on the relationship between A13-DA activity and fine forelimb movements, A13-DA photometry signals were measured while rats handled and manipulated dried vermicelli fragments. This task is known as the vermicelli pasta handling test,[34] and it requires no learning since rats naturally use their paws and fingers to guide a dried vermicelli fragment into their mouth for consumption. Consistent with the reaching task results, A13-DA activity increased when rats picked up

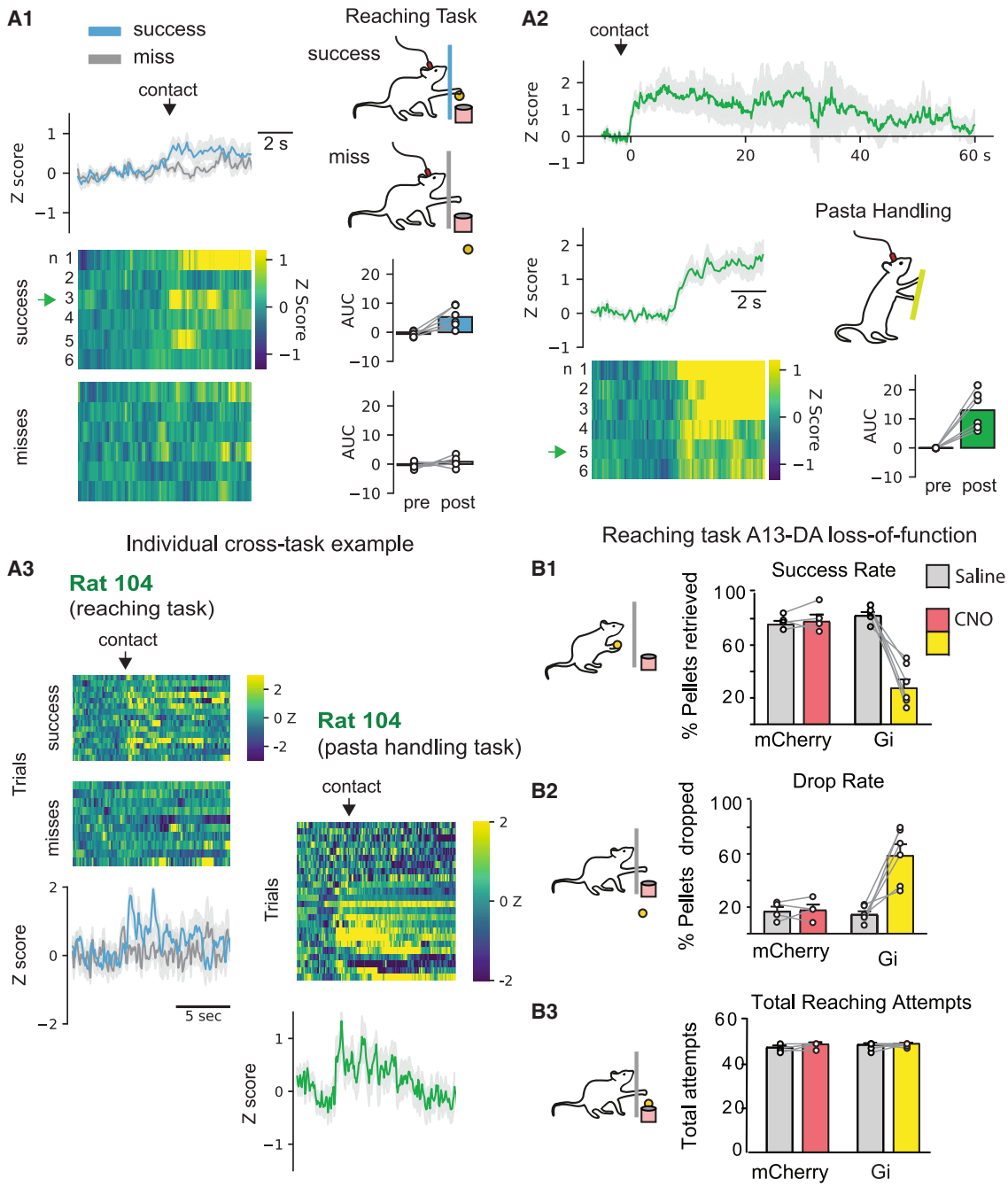

Figure 3. A13-DA activity is related to and is necessary for fine forelimb actions

(A) Compared with baseline, A13-DA population activity increased with successful grasping and handling of sucrose pellets, whereas failed attempts were unrelated to A13-DA activity (A1). (A2) A13-DA activity was elevated while rats handled and manipulated a dried vermicelli fragment. (A3) Response profile of an individual rat across reaching and pasta handling tasks.

(B) Pellet retrieval success rate decreased with A13-DA neuronal inactivation (B1), whereas the total amount of pellets dropped increased (B2). (B3) No change in total reaching attempts was seen following A13-DA inactivation. "Contact" corresponds to contact with the pellet/vermicelli. % pellets retrieved = pellets retrieved/pellets contacted; % pellets dropped = pellets dropped/pellets handled.

Error bars represent the SEM. Green arrows in (A1) and (A2) indicate rats depicted in cross-task individual trials (A3). AUC, area under the curve; CNO, clozapine N-oxide.

Related to Figure S2.

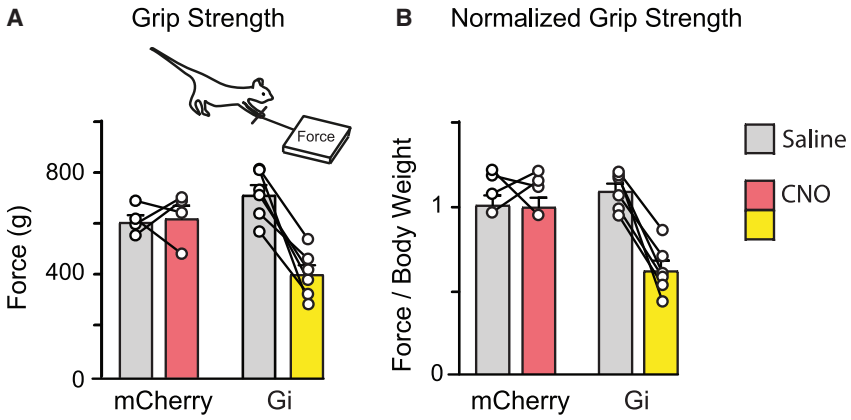

Figure 4. A13-DA inactivation led to a reduction in grip strength

Grip strength was significantly reduced following A13-DA inactivation when measured in total exerted force (A) and when calculated as a function of body weight (B). Error bars represent the SEM.

and handled a dried vermicelli fragment (paired t test: p = 0.004; AUC: baseline, −0.05 ± 0.02; handling, 12.96 ± 2.68; n = 6) (Figure 3A2). The activity was elevated throughout handling, further supporting the idea that A13-DA neurons are important for actions involving fine forelimb movements.

Using a loss-of-function DREADD approach, we next tested whether A13-DA inhibition would impact the rats' ability to successfully reach and grab sucrose pellets. Indeed, inactivating A13-DA neurons in Gi-expressing rats resulted in a significant decrease in the amount of successfully retrieved pellets when animals were injected with CNO compared with both CNO-injected mCherry (n = 4) and saline-injected Gi rats (n = 6) (two-way ANOVA; group, F(1,8) = 26.20, p = 0.0009; saline/CNO, F(1,8) = 24.27, p = 0.001; interaction, F (1,8) = 28.56, p = 0.0007) (Figure 3B1). This retrieval deficit can be partially attributed to an inability to hold onto the pellet since CNO-injected Gi rats showed an increase in pellets reached for, grabbed, but then dropped compared with control animals (two-way ANOVA; group, F(1,8) = 12.11, p = 0.008; saline/CNO, F(1,8) = 13.04, p = 0.007; interaction, F(1,8) = 11.87, p = 0.009) (Figure 3B2). Interestingly, despite showing a strong deficit in retrieving sucrose pellets, CNO-injected Gi rats made a similar amount of reach attempts compared with control conditions, demonstrating that motivation for the reward was intact (two-way ANOVA; group, F(1,8) = 1.371, p = 0.28; saline/CNO, F(1,8) = 2.23, p = 0.17; interaction, F(1,8) = 0.56, p = 0.48) (Figure 3B3). To test whether these deficits were possibly due to changes in nociception or general motor deficits, we next measured locomotor activity and exploration of Gi rats in an open-field chamber. Compared with controls (n = 4) and saline-injected rats, CNO-injected Gi rats (n = 6) showed differences in neither total distance traveled (two-way ANOVA; group, F(1,8) = 0.34, p = 0.58; saline/CNO, F(1,8) = 0.25, p = 0.63; interaction, F(1,8) = 0.12, p = 0.74) (Figure S2A) nor time spent in the arena's center (two-way ANOVA; group, F(1,8) = 0.16, p = 0.70; saline/CNO, F(1,8) = 0.015, p = 0.91; interaction, F(1, 8) = 1.39×10^{-6}, p = 0.99) (Figure S2B). Post-mortem analyses in 4 animals showed that 82.2% of 566 virally infected A13 neurons also expressed TH, whereas more than half (58.8%) of 621 A13-TH+ cells also expressed Gi.

A13-DA neurons contribute to grip strength

The above results are based on behavioral tasks where a forelimb movement led to a reward. In most of the tasks tested, A13-DA activity was seen to increase when animals made a successful movement-reward action. To investigate prehensile actions that are independent of a food reward, we tested rats on a grip strength test. Here, rats were required to hold onto a T-bar connected to a force meter while being gently pulled in the opposite direction. The amount of force rats could exert before letting go of the bar was then measured. CNO-injected Gi rats showed an approximately 60% decrease in grip strength compared with control conditions as measured in grams (two-way ANOVA; group, F(1,8) = 1.63, p = 0.23; saline/CNO, F(1,8) = 14.24, p = 0.004; interaction, F(1,8) = 17.06, p = 0.003) (Figure 4A) but also when force was controlled for body weight (two-way ANOVA; group, F(1,8) = 7.34, p = 0.03; saline/CNO, F (1,8) = 17.30, p = 0.003; interaction, F (1,8) = 16.91, p = 0.003) (Gi, n = 6; mCherry, n = 4) (Figure 4B). Taken together, these data indicate that the contribution of A13-DA activity to fine forelimb motor movements is at least partially due to its involvement in applying adequate levels of grip force for grasping actions.

A13-DA cell ablation severely disrupts pellet handling and grip strength

DA cell degeneration linked to human diseases and their corresponding animal models has been shown to significantly disrupt grasping and handling behavior.[35–38] To shed light on the potential contribution of A13-DA neurons to grasping and handling behavior in a rodent neurodegenerative model, we next investigated the impact of A13-DA neuronal ablation on the reaching/grasping task. In a separate group of well-trained TH-Cre rats, a Cre-dependent viral construct expressing the apoptotic protein caspase-3 was injected into the A13. Pellet retrieval and drop rate were monitored for 20 days post-surgery, and pellet retrieval was seen to progressively decrease and plateau at approximately day 15 (retrieval rate: two-way ANOVA; group, F(1,11) = 57.51, p < 0.0001; day, F(14,153) = 20.65, p < 0.0001; interaction, F(14,153) = 15.42, p < 0.0001; Šidák post hoc differences, days 8–20) (Figure 5A1). Concurrently, pellet drop rate increased across a similar time course (drop rate: two-way ANOVA; group, F(1,11) = 13.18, p = 0.004; day, F(14, 153) = 5.26, p < 0.0001; interaction, F(14, 153) = 4.02, p < 0.0001; Šidák post hoc differences, days 9–20) (caspase, n = 7; GFP, n = 6) (Figure 5A2). Together, these findings demonstrate a striking deficit on a well-learned pellet handling and retrieval task following A13-DA ablation. Furthermore, measurements for total reach attempts revealed an interaction between the group and days, which post hoc comparisons revealed was due to a significant difference on the first test day following surgery (two-way ANOVA; group, F(1,11) = 0.21, p = 0.65; day, F(14,153) = 1.68, p = 0.07; interaction, F(14,153) = 1.97, p = 0.024; Šidák post hoc difference, day 1)

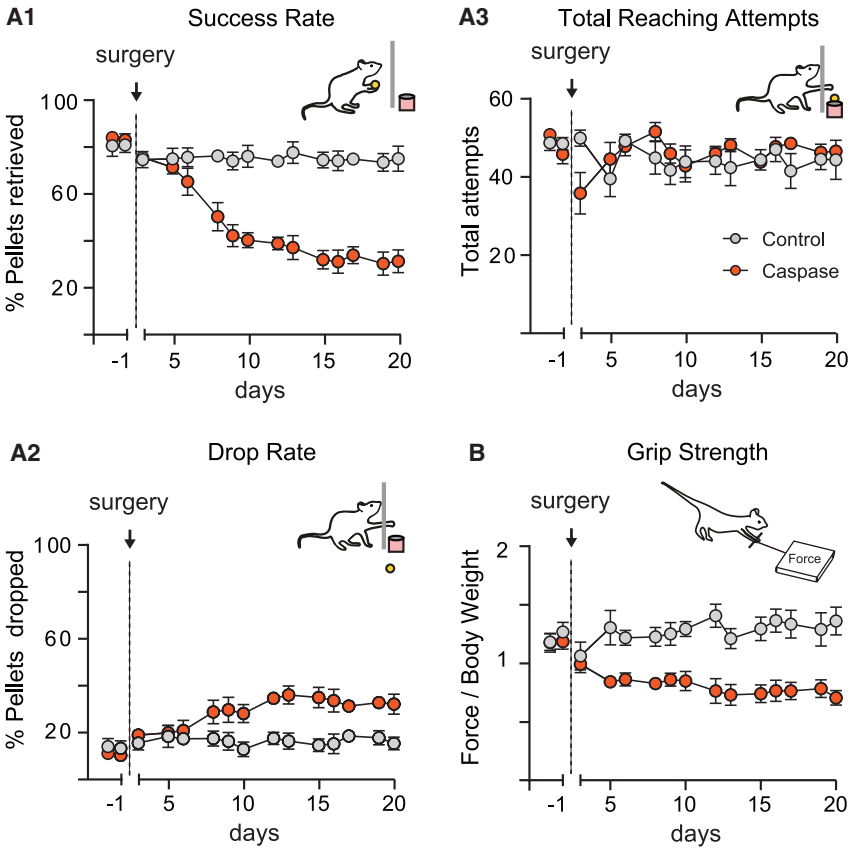

Figure 5. A13-DA ablation adversely impacted fine forelimb motor abilities

(A) When tested in the reaching/grasping task, A13-DA caspase-mediated ablation led to a reduction in % of pellets retrieved (A1) and increase in pellets dropped (A2) while having no impact on total reaching attempts (A3).

(B) Grip strength as a function of body weight was significantly reduced following A13-DA ablation. Error bars represent the SEM.

(Figure 5A3). On subsequent days, there were no significant differences. When next measuring grip strength, A13-DA-ablated caspase rats showed comparable results to those measured in CNO-injected Gi rats where grip strength significantly decreased and plateaued a week following injection to approximately 60% of baseline (force: two-way ANOVA; group, $F(1,11) = 88.73$, $p < 0.0001$; day, $F(15,164) = 1.910$, $p = 0.025$; interaction, $F(15,164) = 6.014$, $p < 0.0001$) (force/BW: two-way ANOVA; group, $F(1,6) = 22.40$, $p = 0.003$; day, $F(15,90) = 2.104$, $p = 0.016$; interaction, $F(15,73) = 5.75$, $p < 0.0001$) (Figure 5B).

A13 TH-expressing neurons project to the RFs and to the SC

We next investigated whether A13-DA axons are positioned to influence descending reach-to-grasp networks. Previous research has shown that neurons in the MDv division of the reticular formation (RF) are important for grasping actions.[39,40] To shed light on whether A13-DA neurons may contribute to MDv-mediated forelimb movements, we next injected a cre-dependent viral tracer (AAV2-dio-EF1a-ChR2(H/R)-eYFP-WPRE) that has previously been shown to mediate both anterograde and retrograde gene transduction[41,42] into the MDv of TH-Cre rats. MDv injections retrogradely labeled TH+ neurons in the caudal division of the A13 (Figure 6A1). On average, MDv injections resulted in 11 ± 1 (n = 4) retrogradely labeled TH+ A13 neurons. We next performed similar injections into the SC, which has been shown to play an important role in prey-directed forelimb movements.[28] SC injections resulted in 25 ± 5 (n = 5) double-labeled A13 neurons (Figure 6A2). These results are in agreement with a previous study demonstrating that A13-TH+ neurons send axons to the SC.[24] RF-projecting A13-TH neurons were located mostly in the caudal division of the A13 (Figure 6A3, top), whereas those projecting to the SC were located rostrally in the A13 (Figure 6A3, bottom), suggesting for separate functional domains by which A13-DA neurons can impact descending reach-to-grasp circuits.

To further characterize A13 projections to the SC and RF, we next directly transfected A13-TH cell bodies with the same cre-dependent virus, which also robustly labeled A13-TH axonal fibers (Figure 6B1) (n = 3). Our anterograde axonal analyses confirmed and extended the retrograde tracing, demonstrating both SC and RF projecting A13-TH axons that heavily innervated the deep gray cell layer of the SC (DpG) that were also seen to extend into the intermediate nucleus of the RF (IRt) (Figures 6B2 and 6B3, respectively). Consistent with previous results[23] there were no axons found in the striatum (Figures S3B1–S3B4), indicating that the contribution of A13-DA neurons to prehensile actions may be independent of striatal motor circuits. To verify that these DpG-SC and IRt-RF projections were indeed arising from A13-TH neurons, we analyzed whether adjacent TH-expressing cell populations also expressed virally expressed GFP and found that DA A9 (VTA), A10 (SNr), and A12, which is located ventrally at the same rostral-caudal level as the A13, were all devoid of GFP (Figures S3A1–S3A4).

DISCUSSION

The above findings indicate that A13-DA activity relates to and is necessary for grasping and handling of objects. Motor forelimb actions such as unrewarded and rewarded CP were tightly linked to A13-DA population activity, as were skilled learned and unlearned grasping and handling movements. Self-administration of palatable liquid rewards showed no relation to A13-DA activity, and manipulations of A13-DA neurons did not impact motivation to LP for rewards. In fact, despite the severe deficits in successfully grabbing and retrieving sucrose pellets resulting from A13-DA neuro-inactivation or degeneration motivation for rewards was intact. The diminished ability to successfully retrieve pellets coincided instead with an increase in pellets

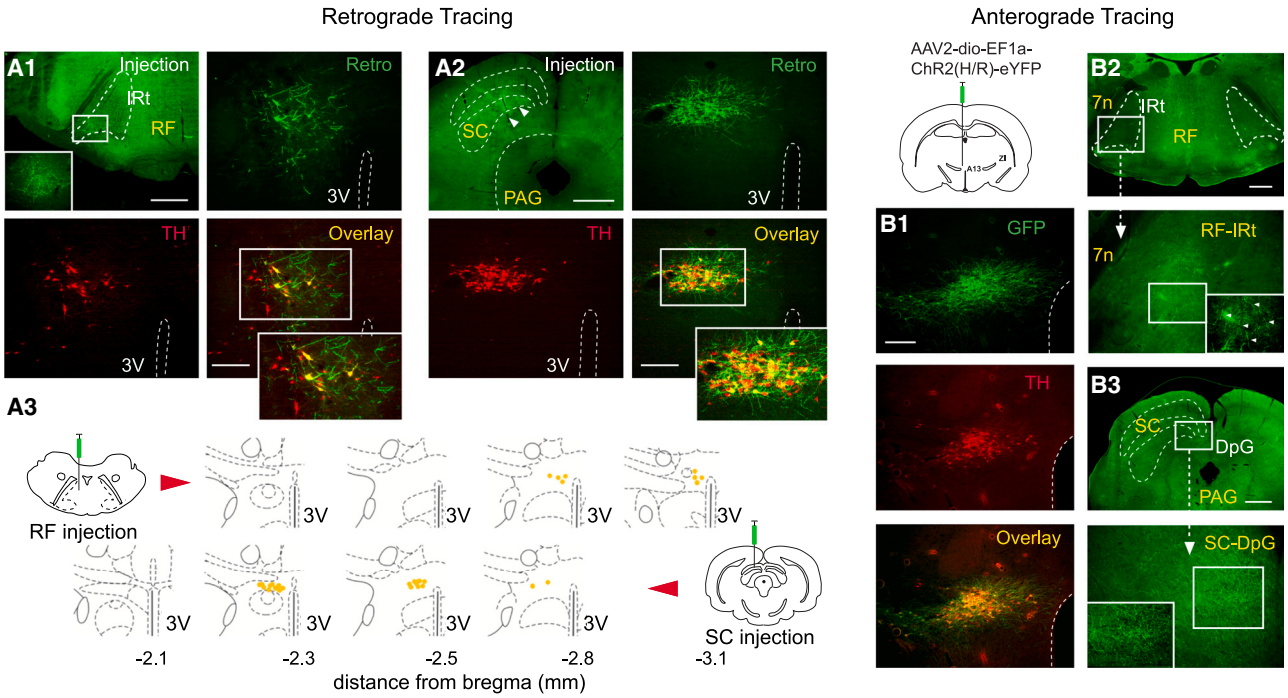

Figure 6. A13-TH projects to the superior colliculus and reticular formation

(A) Retrograde labeling of A13-TH+ neurons projecting to the RF and SC. Retrograde viral tracer injections into the RF (A1) labeled A13 neurons (retro) that express TH, which was verified using immunocytochemical methods for labeling TH. Similar injections into the SC (A2) labeled A13 TH-expressing neurons. (A3) Distribution of retrogradely double-labeled A13 neurons (yellow dots) following injections into the reticular formation (top) or SC (bottom) from a single animal. (B) Anterograde labeling of A13-TH neurons. (B1) Colocalization of viral expression and TH in A13 neurons and their axonal projections to the DpG layer of the SC (B2) and IRt division of the RF (B3).

IRt, intermediate nucleus of the RF; DpG, deep gray cell layer of the SC; PAG, periaqueductal gray; 3V, 3rd ventricle; 7n, facial nerve. Scale bars, 1 mm in (A1), (A2) (top left), (B2), and (B3); 200 μm in (A1), (A2) (retro, TH, overlay), and (B1).

Related to Figure S3.

dropped and a reduction in grip strength, indicating that A13-DA activity is necessary for controlling paw and finger movements that are largely associated with prehensile actions. A13-DA neurons were also shown to project to the RF and the SC, both of which are regions previously shown to be involved in coordinating reach-to-grasp movements.

A13-DA neurons encode for prehensile actions that are uncoupled from motivation for reward

In rodents, SFMs constitute a series of precisely timed sub-movements where the forelimb outwardly extends and is completed by the paw and digits enclosing around a target object. DA cell activity is well known to be critical for the planning and execution of complex motor sequences, including SFMs,[32,43] and has been shown to contribute in varying degrees to the different sub-components that make up a coordinated motor response. For instance, DA cell activity has been associated with action planning and initiation,[14,44,45] movement velocity,[12,46] force,[15,47] locomotion,[20,48] and the acquisition of learned skilled movements.[49,50] Such a multi-faceted involvement for DA cell activity in movements consequently makes it difficult to target the exact contribution of DA activity on SFMs, especially since separate DA populations have been shown to impact different SFM sub-movements through dissimilar pathways.[35,43,50,51] Our findings are the first to show a specific involvement of the A13-DA neuronal population in SFMs. In addition to disruptions in prehensile actions, increases in A13-DA activity were time-locked to grasping and were maintained while animals handled a pasta fragment, indicating that this dopaminergic population plays a specialized role in executing and maintaining grasping/handling movements. Our analyses, however, were unable to delineate which, if any in particular, prehensile sub-movements are encoded by A13-DA activity, except that grip strength was severely impacted by A13-DA disruption. A future, more systematic analysis of the underlying sub-movements and A13-DA activity will help reveal the precise A13-DA contribution to SFMs.

Prominent theories of DA function are based on the principle that DA-related motor functions and motivation are functionally coupled so that organisms can effectively plan, initiate, and execute motor programs to realize a goal.[16,52,53] This idea is highlighted by a study by Mazzoni et al.,[54] where bradykinesia—a DA-dependent slowing of motor movements—in Parkinson's disease (PD) patients was shown to be at least partially attributed to a reluctance to move quickly rather than a deficit in motor speed or accuracy. This is in line with other work showing that the amount of vigor—defined as the speed, frequency, and amplitude of movements[55]—at the onset of a planned action is strongly related to DA activity and determined by the predictability or incentive value of the goal.[15,56–59] Our

results indicate that movement-related A13-DA activity is unrelated to reward or reward consumption. Furthermore, it is unlikely to be associated with vigor since A13-DA activity was related to paw actions that occurred at the end of reach-to-grasp movements and was unrelated to similar movements that ended in failed reaching attempts. Moreover, inactivation/neurodegeneration of A13-DA neurons had no impact on LP or total reaching attempts, indicating that motivation and, as a consequence, motor planning and initiation were intact. These results demonstrate a role for A13-DA neurons in SFMs that is uncoupled from the motivational factors that drive specific prehensile actions.

Descending A13 projections innervate sensorimotor regions in the midbrain

Our tracing results are in agreement with previous work demonstrating A13-DA inputs to the SC.[24] The SC is a midbrain region important for coordinating movements toward or away from salient stimuli[27,28] and has been shown to promote orienting responses by, among other mechanisms, transforming visual and somatosensory information into saccadic responses that align with head rotations so as to stabilize gaze.[60,61] Interestingly, in both human and non-human primates, SC circuits have been shown to also encode for reaching movements.[62,63] In one study, neurons in intermediate and deep layers of the primate SC were active during reaching movements and increased in activity when combined with visual input suggesting that specific SC circuits may be involved in gaze anchoring for the purpose of reaching and grasping target objects.[64] In line with the current results, intermediate and deep layer SC neurons have been shown to respond when monkeys made contact with a target object but only sparingly or not at all during the reaching movement.[65] Less is known regarding SC and reach-to-grasp movements in rodents, but related work has shown that SC microcircuits in mice are important in predatory hunting where a well-orchestrated repertoire of eye, head, body, and forelimb movements are necessary for effective hunting—the end result being a well-timed reaching and grasping attack.[28] Recent circuit mapping work has demonstrated that ZI circuits are also necessary for such prey-directed movements, revealing a potential local A13-DA contribution to prey-grasping[66] that in conjunction with sensorimotor responses in intermediate and deep layers of the SC may help coordinate effective predatory hunting.[28]

Functional architecture of brainstem-mediated SFMs

SFM motor sequences have been shown to be generated cortically[67] and relayed to the spinal cord through direct descending cortico-spinal projections and indirectly via the RF, where pathways diverge innervating spinal circuits via the tectospinal, rubrospinal, and reticulospinal tracts.[68] Recent work has shown that functional divisions exist within the RF where separate subregions regulate distinct SFM motor components. For example, when tested on a reaching task, mice whose lateral RF glutamatergic cells were ablated showed deficits in reaching such that they consistently overreached, missing the endpoint.[40] Conversely, selective degeneration of medial RF glutamatergic neurons specifically affected pellet grasping, leaving reaching behavior intact.[39] Grip strength was unaffected in either study, suggesting that these RF subregions are important for coordinating SFMs rather than generating the appropriate force necessary for grasping target objects. These functional RF divisions seem to be due in part to parallel reaching and grasping information that is transmitted from the anterior cortex to the RF that is topographically organized in a lateral/medial to RF dorsal/ventral functional map, respectively.[69] Our results demonstrating that A13-DA neurons mostly terminate in the reaching-related more ventrally located IRt indicate that A13-DA inputs to the RF may have a role to play in the integration of reaching information that ultimately results in successful grasping actions. Previous anatomical work has shown that A13 neurons innervate the RF, specifically the gigantocellular nucleus, but these projections were shown to be from non-TH-expressing A13 neurons.[23] The current results demonstrate an A13-DA to RF projection thus revealing an anatomical substrate by which A13-DA neurons can modulate RF reach-to-grasp computations. Future research investigating the functional impact of A13-DA terminals onto RF circuits will be an important next step in determining the neural mechanisms for coordinating effective SFMs.

Dopaminergic cell activity is important for reaching and grasping movements

Reach-to-grasp actions are well known to be symptomatic of DA neurodegenerative diseases and of their corresponding animal models.[35,70–74] For instance, detailed kinematic analyses of reach-to-grasp motions in PD and Huntington's disease (HD) patients have shown greater trial-to-trial variability in reaching for and grasping a target object compared with healthy individuals.[75–78] These deficits may result from an inability to shape appropriate anticipatory hand movements[78,79] and also, in some cases, from alterations in the ability to apply the appropriate force[75,80,81] (but see also Jordan et al.[82] and Nowak and Hermsdörfer[83]). Similar deficits in grasping have recently been linked to PD disease progression[37] and, from a therapeutic standpoint, have been shown to be an effective diagnostic predictor of PD in early stages of the disease.[84,85] Surprisingly, pharmacotherapies for treating PD have been shown to be only partially effective in reversing PD-SFM symptomology.[79,86] For example, an analysis of hand kinematics in PD patients on/off L-Dopa therapy showed that reaching actions in medicated patients were only slightly improved, whereas improvements in grasping were negligible.[87] On the other hand, surgical therapies such as deep brain stimulation of the subthalamic nucleus—a region in close proximity to the A13—show significant benefits in remediating both PD reaching and grasping deficits.[88,89] Such results suggest that separate mechanisms are at play for the different phases of SFMs that are circuit-specific and/or DA-dependent.

Hand actions are critically important in our daily lives. Everyday tasks such as cooking, eating, dressing, and even holding playing cards are severely impacted in PD patients,[90] which consequently affects their physical and mental well being.[91,92] Our results demonstrate a clear and important role for A13-DA neurons in prehensile actions. From our analysis, it is unclear, however, what signals are encoded by A13-DA circuits, the mechanisms by which DA or A13-DA co-transmitters might impact target regions, and whether this distinct central DA population is affected in PD and HD. As such, future research investigating the contribution of this DA population to motor

coordination and execution will be critical for positioning the A13 within the functional framework of central DA motor circuits and their relation to DA neurodegenerative diseases.

STAR★METHODS

Detailed methods are provided in the online version of this paper and include the following:

- KEY RESOURCES TABLE
- RESOURCE AVAILABILITY
  - Lead contact
  - Materials availability
  - Data and code availability
- EXPERIMENTAL MODEL AND STUDY PARTICIPANT DETAILS
- METHOD DETAILS
  - Virus injection and implant surgery
  - Fiber photometry
  - Histology
  - Behavioral Paradigms
- QUANTIFICATION AND STATISTICAL ANALYSIS

SUPPLEMENTAL INFORMATION

Supplemental information can be found online at https://doi.org/10.1016/j.cub.2023.09.044.

ACKNOWLEDGMENTS

The authors acknowledge the help and support from the staff of the Division of Biomedical Services, Preclinical Research Facility, University of Leicester for technical support and the care of experimental animals, as well as Dr. Todor Gerdjikov and colleagues in the Department of Neuroscience, Psychology, and Behavior at the University of Leicester for their academic contribution. This work was funded by Wellcome (grant #209023/Z/17/Z to J.A.-S. and WT ISSF Early Career Research Fellowship to C.G.) and the Leverhulme Trust (grant #RPG-2017-417 to J.E.M. and J.A.-S.).

AUTHOR CONTRIBUTIONS

Conceptualization, C.G. and J.A.-S.; formal analysis, C.G., J.E.M., J.A.-S., J.H., and G.C.; investigation, G.C., J.H., J.A.-S., and C.G.; writing – original draft, J.A.-S. and C.G.; writing – review & editing, J.A.-S., J.E.M., C.G., G.C., and J.H.; funding acquisition, J.A.-S., J.E.M., and G.C.

DECLARATION OF INTERESTS

The authors declare no competing interests.

INCLUSION AND DIVERSITY

We support inclusive, diverse, and equitable conduct of research.

Received: December 14, 2022
Revised: August 14, 2023
Accepted: September 18, 2023
Published: October 9, 2023

REFERENCES

1. Hefter, H., Hömberg, V., Lange, H.W., and Freund, H.J. (1987). Impairment of rapid movement in Huntington's disease. Brain *110*, 585–612.
2. Oyanagi, K., Takeda, S., Takahashi, H., Ohama, E., and Ikuta, F. (1989). A quantitative investigation of the substantia nigra in Huntington's disease. Ann. Neurol. *26*, 13–19.
3. Fearnley, J.M., and Lees, A.J. (1991). Ageing and Parkinson's disease: substantia nigra regional selectivity. Brain *114*, 2283–2301.
4. Gerlach, M., and Riederer, P. (1996). Animal models of Parkinson's disease: an empirical comparison with the phenomenology of the disease in man. J. Neural Transm. (Vienna) *103*, 987–1041.
5. Chaudhuri, K.R., Healy, D.G., and Schapira, A.H.; National Institute for Clinical Excellence (2006). Non-motor symptoms of Parkinson's disease: diagnosis and management. Lancet Neurol. *5*, 235–245.
6. Jankovic, J. (2008). Parkinson's disease: clinical features and diagnosis. J. Neurol. Neurosurg. Psychiatry *79*, 368–376.
7. Hokfelt, T. (1984). Distribution maps of tyrosine-hydroxylase-immunoreactive neurons in the rat brain. In Handbook of Chemical Neuroanatomy, Vol. 2, A. Björklund, and T. Hökfelt, eds. (Elsevier), pp. 277–379.
8. Björklund, A., and Dunnett, S.B. (2007). Dopamine neuron systems in the brain: an update. Trends Neurosci. *30*, 194–202.
9. Schultz, W., Apicella, P., and Ljungberg, T. (1993). Responses of monkey dopamine neurons to reward and conditioned stimuli during successive steps of learning a delayed response task. J. Neurosci. *13*, 900–913.
10. Fiorillo, C.D., Tobler, P.N., and Schultz, W. (2003). Discrete coding of reward probability and uncertainty by dopamine neurons. Science *299*, 1898–1902.
11. Lak, A., Stauffer, W.R., and Schultz, W. (2014). Dopamine prediction error responses integrate subjective value from different reward dimensions. Proc. Natl. Acad. Sci. USA *111*, 2343–2348.
12. Panigrahi, B., Martin, K.A., Li, Y., Graves, A.R., Vollmer, A., Olson, L., Mensh, B.D., Karpova, A.Y., and Dudman, J.T. (2015). Dopamine is required for the neural representation and control of movement vigor. Cell *162*, 1418–1430.
13. Howard, C.D., Li, H., Geddes, C.E., and Jin, X. (2017). Dynamic nigrostriatal dopamine biases action selection. Neuron *93*, 1436–1450.e8.
14. da Silva, J.A., Tecuapetla, F., Paixão, V., and Costa, R.M. (2018). Dopamine neuron activity before action initiation gates and invigorates future movements. Nature *554*, 244–248.
15. Hughes, R.N., Bakhurin, K.I., Petter, E.A., Watson, G.D.R., Kim, N., Friedman, A.D., and Yin, H.H. (2020). Ventral tegmental dopamine neurons control the impulse vector during motivated behavior. Curr. Biol. *30*, 2681–2694.e5.
16. Berridge, K.C. (2007). The debate over dopamine's role in reward: the case for incentive salience. Psychopharmacology *191*, 391–431.
17. Grace, A.A., Floresco, S.B., Goto, Y., and Lodge, D.J. (2007). Regulation of firing of dopaminergic neurons and control of goal-directed behaviors. Trends Neurosci. *30*, 220–227.
18. Kobayashi, S., and Schultz, W. (2008). Influence of reward delays on responses of dopamine neurons. J. Neurosci. *28*, 7837–7846.
19. Palmiter, R.D. (2008). Dopamine signaling in the dorsal striatum is essential for motivated behaviors: lessons from dopamine-deficient mice. Ann. N. Y. Acad. Sci. *1129*, 35–46.
20. Koblinger, K., Jean-Xavier, C., Sharma, S., Füzesi, T., Young, L., Eaton, S.E.A., Kwok, C.H.T., Bains, J.S., and Whelan, P.J. (2018). Optogenetic activation of A11 region increases motor activity. Front. Neural Circuits *12*, 86.
21. Zhang, X., and van den Pol, A.N. (2016). Hypothalamic arcuate nucleus tyrosine hydroxylase neurons play orexigenic role in energy homeostasis. Nat. Neurosci. *19*, 1341–1347.
22. Negishi, K., Payant, M.A., Schumacker, K.S., Wittmann, G., Butler, R.M., Lechan, R.M., Steinbusch, H.W.M., Khan, A.M., and Chee, M.J. (2020). Distributions of hypothalamic neuron populations coexpressing tyrosine hydroxylase and the vesicular GABA transporter in the mouse. J. Comp. Neurol. *528*, 1833–1855.

23. Sharma, S., Kim, L.H., Mayr, K.A., Elliott, D.A., and Whelan, P.J. (2018). Parallel descending dopaminergic connectivity of A13 cells to the brainstem locomotor centers. Sci. Rep. *8*, 7972.

24. Bolton, A.D., Murata, Y., Kirchner, R., Kim, S.-Y., Young, A., Dang, T., Yanagawa, Y., and Constantine-Paton, M. (2015). A diencephalic dopamine source provides input to the superior colliculus, where D1 and D2 receptors segregate to distinct functional zones. Cell Rep. *13*, 1003–1015.

25. Cohen, J.D., and Castro-Alamancos, M.A. (2010). Neural correlates of active avoidance behavior in superior colliculus. J. Neurosci. *30*, 8502–8511.

26. Zingg, B., Chou, X.L., Zhang, Z.G., Mesik, L., Liang, F., Tao, H.W., and Zhang, L.I. (2017). AAV-mediated anterograde transsynaptic tagging: mapping corticocollicular input-defined neural pathways for defense behaviors. Neuron *93*, 33–47.

27. Evans, D.A., Stempel, A.V., Vale, R., Ruehle, S., Lefler, Y., and Branco, T. (2018). A synaptic threshold mechanism for computing escape decisions. Nature *558*, 590–594.

28. Shang, C., Liu, A., Li, D., Xie, Z., Chen, Z., Huang, M., Li, Y., Wang, Y., Shen, W.L., and Cao, P. (2019). A subcortical excitatory circuit for sensory-triggered predatory hunting in mice. Nat. Neurosci. *22*, 909–920.

29. Huang, M., Li, D., Cheng, X., Pei, Q., Xie, Z., Gu, H., Zhang, X., Chen, Z., Liu, A., and Wang, Y. (2021). The tectonigral pathway regulates appetitive locomotion in predatory hunting in mice. Nat. Commun. *12*, 1–17.

30. Arnold, J.M., and Roberts, D.C. (1997). A critique of fixed and progressive ratio schedules used to examine the neural substrates of drug reinforcement. Pharmacol. Biochem. Behav. *57*, 441–447.

31. Aitta-aho, T., Phillips, B.U., Pappa, E., Hay, Y.A., Harnischfeger, F., Heath, C.J., Saksida, L.M., Bussey, T.J., and Apergis-Schoute, J. (2017). Accumbal cholinergic interneurons differentially influence motivation related to satiety signaling. eNeuro *4*, ENEURO.0328-16.2017.

32. Whishaw, I.Q., and Pellis, S.M. (1990). The structure of skilled forelimb reaching in the rat: a proximally driven movement with a single distal rotatory component. Behav. Brain Res. *41*, 49–59.

33. Lammel, S., Steinberg, E.E., Földy, C., Wall, N.R., Beier, K., Luo, L., and Malenka, R.C. (2015). Diversity of transgenic mouse models for selective targeting of midbrain dopamine neurons. Neuron *85*, 429–438.

34. Tennant, K., Asay, A., Allred, R., Ozburn, A., Kleim, J., and Jones, T. (2010). The vermicelli and capellini handling tests: simple quantitative measures of dexterous. J. Vis. Exp.2076

35. Miklyaeva, E.I., Castañeda, E., and Whishaw, I.Q. (1994). Skilled reaching deficits in unilateral dopamine-depleted rats: impairments in movement and posture and compensatory adjustments. J. Neurosci. *14*, 7148–7158.

36. Dunnett, S.B., Torres, E.M., and Annett, L.E. (1998). A lateralised grip strength test to evaluate unilateral nigrostriatal lesions in rats. Neurosci. Lett. *246*, 1–4.

37. Roberts, H.C., Syddall, H.E., Butchart, J.W., Stack, E.L., Cooper, C., and Sayer, A.A. (2015). The association of grip strength with severity and duration of Parkinson's: a cross-sectional study. Neurorehab. Neural Repair *29*, 889–896.

38. Thomas, M., Lenka, A., and Kumar Pal, P. (2017). Handwriting analysis in Parkinson's disease: current status and future directions. Mov. Disord. Clin. Pract. *4*, 806–818.

39. Esposito, M.S., Capelli, P., and Arber, S. (2014). Brainstem nucleus MdV mediates skilled forelimb motor tasks. Nature *508*, 351–356.

40. Ruder, L., Schina, R., Kanodia, H., Valencia-Garcia, S., Pivetta, C., and Arber, S. (2021). A functional map for diverse forelimb actions within brainstem circuitry. Nature *590*, 445–450.

41. McCall, J.G., Siuda, E.R., Bhatti, D.L., Lawson, L.A., McElligott, Z.A., Stuber, G.D., and Bruchas, M.R. (2017). Locus coeruleus to basolateral amygdala noradrenergic projections promote anxiety-like behavior. eLife *6*, e18247.

42. Rothermel, M., Brunert, D., Zabawa, C., Díaz-Quesada, M., and Wachowiak, M. (2013). Transgene expression in target-defined neuron populations mediated by retrograde infection with adeno-associated viral vectors. J. Neurosci. *33*, 15195–15206.

43. Bova, A., Gaidica, M., Hurst, A., Iwai, Y., Hunter, J., and Leventhal, D.K. (2020). Precisely timed dopamine signals establish distinct kinematic representations of skilled movements. eLife *9*, e61591.

44. Owen, A.M., Sahakian, B.J., Hodges, J.R., Summers, B.A., Polkey, C.E., and Robbins, T.W. (1995). Dopamine-dependent frontostriatal planning deficits in early Parkinson's disease. Neuropsychology *9*, 126–140.

45. Syed, E.C., Grima, L.L., Magill, P.J., Bogacz, R., Brown, P., and Walton, M.E. (2016). Action initiation shapes mesolimbic dopamine encoding of future rewards. Nat. Neurosci. *19*, 34–36.

46. Lofredi, R., Neumann, W.J., Bock, A., Horn, A., Huebl, J., Siegert, S., Schneider, G.H., Krauss, J.K., and Kühn, A.A. (2018). Dopamine-dependent scaling of subthalamic gamma bursts with movement velocity in patients with Parkinson's disease. eLife *7*, e31895.

47. Park, J., Lewis, M.M., Huang, X., and Latash, M.L. (2014). Dopaminergic modulation of motor coordinaton in Parkinson's disease. Parkinsonism Relat. Disord. *20*, 64–68.

48. Kelly, V.E., Eusterbrock, A.J., and Shumway-Cook, A. (2012). A review of dual-task walking deficits in people with Parkinson's disease: motor and cognitive contributions, mechanisms, and clinical implications. Parkinsons Dis. *2012*, 918719.

49. Molina-Luna, K., Pekanovic, A., Röhrich, S., Hertler, B., Schubring-Giese, M., Rioult-Pedotti, M.-S., and Luft, A.R. (2009). Dopamine in motor cortex is necessary for skill learning and synaptic plasticity. PLoS One *4*, e7082.

50. Kawashima, S., Ueki, Y., Kato, T., Matsukawa, N., Mima, T., Hallett, M., Ito, K., and Ojika, K. (2012). Changes in striatal dopamine release associated with human motor-skill acquisition. PLoS One *7*, e31728.

51. Barnéoud, P., Parmentier, S., Mazadier, M., Miquet, J.M., Boireau, A., Dubédat, P., and Blanchard, J.C. (1995). Effects of complete and partial lesions of the dopaminergic mesotelencephalic system on skilled forelimb use in the rat. Neuroscience *67*, 837–848.

52. Niv, Y., Daw, N.D., Joel, D., and Dayan, P. (2007). Tonic dopamine: opportunity costs and the control of response vigor. Psychopharmacology *191*, 507–520.

53. Salamone, J.D., Correa, M., Ferrigno, S., Yang, J.H., Rotolo, R.A., and Presby, R.E. (2018). The psychopharmacology of effort-related decision making: dopamine, adenosine, and insights into the neurochemistry of motivation. Pharmacol. Rev. *70*, 747–762.

54. Mazzoni, P., Hristova, A., and Krakauer, J.W. (2007). Why don't we move faster? Parkinson's disease, movement vigor, and implicit motivation. J. Neurosci. *27*, 7105–7116.

55. Dudman, J.T., and Krakauer, J.W. (2016). The basal ganglia: from motor commands to the control of vigor. Curr. Opin. Neurobiol. *37*, 158–166.

56. Pekny, S.E., Izawa, J., and Shadmehr, R. (2015). Reward-dependent modulation of movement variability. J. Neurosci. *35*, 4015–4024.

57. Hamid, A.A., Pettibone, J.R., Mabrouk, O.S., Hetrick, V.L., Schmidt, R., Vander Weele, C.M., Kennedy, R.T., Aragona, B.J., and Berke, J.D. (2016). Mesolimbic dopamine signals the value of work. Nat. Neurosci. *19*, 117–126.

58. Bogacz, R. (2020). Dopamine role in learning and action inference. eLife *9*, e53262.

59. Michely, J., Viswanathan, S., Hauser, T.U., Delker, L., Dolan, R.J., and Grefkes, C. (2020). The role of dopamine in dynamic effort-reward integration. Neuropsychopharmacology *45*, 1448–1453.

60. Klier, E.M., Wang, H., and Crawford, J.D. (2001). The superior colliculus encodes gaze commands in retinal coordinates. Nat. Neurosci. *4*, 627–632.

61. Zahler, S.H., Taylor, D.E., Wong, J.Y., Adams, J.M., and Feinberg, E.H. (2021). Superior colliculus drives stimulus-evoked directionally biased saccades and attempted head movements in head-fixed mice. eLife *10*, e73081.

62. Himmelbach, M., Linzenbold, W., and Ilg, U.J. (2013). Dissociation of reach-related and visual signals in the human superior colliculus. Neuroimage *82*, 61–67.

63. Song, J.H., and McPeek, R.M. (2015). Neural correlates of target selection for reaching movements in superior colliculus. J. Neurophysiol. *113*, 1414–1422.

64. Reyes-Puerta, V., Philipp, R., Lindner, W., and Hoffmann, K.P. (2010). Role of the rostral superior colliculus in gaze anchoring during reach movements. J. Neurophysiol. *103*, 3153–3166.

65. Nagy, A., Kruse, W., Rottmann, S., Dannenberg, S., and Hoffmann, K.P. (2006). Somatosensory-motor neuronal activity in the superior colliculus of the primate. Neuron *52*, 525–534.

66. Zhao, Z.D., Chen, Z., Xiang, X., Hu, M., Xie, H., Jia, X., Cai, F., Cui, Y., Chen, Z., Qian, L., et al. (2019). Zona incerta GABAergic neurons integrate prey-related sensory signals and induce an appetitive drive to promote hunting. Nat. Neurosci. *22*, 921–932.

67. Turella, L., and Lingnau, A. (2014). Neural correlates of grasping. Front. Hum. Neurosci. *8*, 686.

68. Alstermark, B., and Isa, T. (2012). Circuits for skilled reaching and grasping. Annu. Rev. Neurosci. *35*, 559–578.

69. Yang, W., Kanodia, H., and Arber, S. (2023). Structural and functional map for forelimb movement phases between cortex and medulla. Cell *186*, 162–177.e18.

70. Olsson, M., Nikkhah, G., Bentlage, C., and Björklund, A. (1995). Forelimb akinesia in the rat Parkinson model: differential effects of dopamine agonists and nigral transplants as assessed by a new stepping test. J. Neurosci. *15*, 3863–3875.

71. Majsak, M.J., Kaminski, T., Gentile, A.M., and Flanagan, J.R. (1998). The reaching movements of patients with Parkinson's disease under self-determined maximal speed and visually cued conditions. Brain *121*, 755–766.

72. Whishaw, I.Q., Suchowersky, O., Davis, L., Sarna, J., Metz, G.A., and Pellis, S.M. (2002). Impairment of pronation, supination, and body co-ordination in reach-to-grasp tasks in human Parkinson's disease (PD) reveals homology to deficits in animal models. Behav. Brain Res. *133*, 165–176.

73. Pessiglione, M., Guehl, D., Agid, Y., Hirsch, E.C., Féger, J., and Tremblay, L. (2003). Impairment of context-adapted movement selection in a primate model of presymptomatic Parkinson's disease. Brain *126*, 1392–1408.

74. Jo, H.J., Park, J., Lewis, M.M., Huang, X., and Latash, M.L. (2015). Prehension synergies and hand function in early-stage Parkinson's disease. Exp. Brain Res. *233*, 425–440.

75. Fellows, S., Schwarz, M., Schaffrath, C., Dömges, F., and Noth, J. (1997). Disturbances of precision grip in Huntington's disease. Neurosci. Lett. *226*, 103–106.

76. Alberts, J.L., Saling, M., Adler, C.H., and Stelmach, G.E. (2000). Disruptions in the reach-to-grasp actions of Parkinson's patients. Exp. Brain Res. *134*, 353–362.

77. Gordon, A.M., Quinn, L., Reilmann, R., and Marder, K. (2000). Coordination of prehensile forces during precision grip in Huntington's disease. Exp. Neurol. *163*, 136–148.

78. Lu, C., Bharmal, A., Kiss, Z.H., Suchowersky, O., and Haffenden, A.M. (2010). Attention and reach-to-grasp movements in Parkinson's disease. Exp. Brain Res. *205*, 69–80.

79. Schettino, L.F., Adamovich, S.V., Hening, W., Tunik, E., Sage, J., and Poizner, H. (2006). Hand preshaping in Parkinson's disease: effects of visual feedback and medication state. Exp. Brain Res. *168*, 186–202.

80. Reilmann, R., Kirsten, F., Quinn, L., Henningsen, H., Marder, K., and Gordon, A.M. (2001). Objective assessment of progression in Huntington's disease: a 3-year follow-up study. Neurology *57*, 920–924.

81. Guo, X., Hosseini, N., Hejduková, B., Olsson, T., Johnels, B., and Steg, G. (2004). Load force during manual transport in Parkinson's disease. Acta Neurol. Scand. *109*, 416–424.

82. Jordan, N., Sagar, H.J., and Cooper, J.A. (1992). A component analysis of the generation and release of isometric force in Parkinson's disease. J. Neurol. Neurosurg. Psychiatry *55*, 572–576.

83. Nowak, D.A., and Hermsdörfer, J. (2002). Coordination of grip and load forces during vertical point-to-point movements with a grasped object in Parkinson's disease. Behav. Neurosci. *116*, 837–850.

84. Kandaswamy, D., M, M., Alexander, M., Prabhu, K., S, M.G., and Krothapalli, S.B. (2018). Quantitative assessment of hand dysfunction in patients with early Parkinson's disease and focal hand dystonia. J. Mov. Disord. *11*, 35–44.

85. Saikia, A., Hussain, M., Barua, A.R., and Paul, S. (2018). Detection of Parkinson's disease using clinical diagnostic tools. Stroke *6*, 1143.

86. Tunik, E., Feldman, A.G., and Poizner, H. (2007). Dopamine replacement therapy does not restore the ability of Parkinsonian patients to make rapid adjustments in motor strategies according to changing sensorimotor contexts. Parkinsonism Relat. Disord. *13*, 425–433.

87. Negrotti, A., Secchi, C., and Gentilucci, M. (2005). Effects of disease progression and L-dopa therapy on the control of reaching-grasping in Parkinson's disease. Neuropsychologia *43*, 450–459.

88. Dafotakis, M., Fink, G.R., Allert, N., and Nowak, D.A. (2008). The impact of subthalamic deep brain stimulation on bradykinesia of proximal and distal upper limb muscles in Parkinson's disease. J. Neurol. *255*, 429–437.

89. Pötter-Nerger, M., Habben, A., Herzog, J., Falk, D., Mehdorn, M.H., Deuschl, G., and Volkmann, J. (2013). Kinematic effects of subthalamic stimulation on reach-to-grasp movements in Parkinson's disease. Parkinsonism Relat. Disord. *19*, 32–36.

90. Sjödahl Hammarlund, C., Westergren, A., Åström, I., Edberg, A.K., and Hagell, P. (2018). The impact of living with Parkinson's disease: balancing within a web of needs and demands. Parkinsons Dis. *2018*, 4598651.

91. Kuopio, A.M., Marttila, R.J., Helenius, H., Toivonen, M., and Rinne, U.K. (2000). The quality of life in Parkinson's disease. Mov. Disord. *15*, 216–223.

92. Dissanayaka, N.N., Sellbach, A., Matheson, S., O'Sullivan, J.D., Silburn, P.A., Byrne, G.J., Marsh, R., and Mellick, G.D. (2010). Anxiety disorders in Parkinson's disease: prevalence and risk factors. Mov. Disord. *25*, 838–845.

93. Konanur, V.R., Hsu, T.M., Kanoski, S.E., Hayes, M.R., and Roitman, M.F. (2020). Phasic dopamine responses to a food-predictive cue are suppressed by the glucagon-like peptide-1 receptor agonist Exendin-4. Physiol. Behav. *215*, 112771.

94. Bayley, P.J., Bentley, G.D., Jackson, A., Williamson, D., and Dawson, G.R. (1996). Comparison of benzodiazepine (BZ) receptor agonists in two rodent activity tests. J. Psychopharmacol. *10*, 206–213.

95. Manfré, G., Clemensson, E.K.H., Kyriakou, E.I., Clemensson, L.E., Van der Harst, J.E., Homberg, J.R., and Nguyen, H.P. (2017). The BACHD rat model of Huntington disease shows specific deficits in a test battery of motor function. Front. Behav. Neurosci. *11*, 218.

STAR★METHODS

KEY RESOURCES TABLE

REAGENT or RESOURCE	SOURCE	IDENTIFIER
Antibodies		
mouse anti-tyrosine hydroxylase	Sigma-Merck	Cat#MAB318; RRID: AB_2201528
rabbit anti-mCherry	Abcam, Cambridge, UK	Cat#ab167453; RRID: AB_2571870
chicken anti-GFP	Abcam, Cambridge, UK	Cat#ab13970; RRID: AB_300798
donkey anti-mouse AlexaFluor 488	Abcam, Cambridge, UK	Cat#ab150105; RRID: AB_2732856
donkey anti-Rabbit 594	Abcam, Cambridge, UK	Cat#ab150076; RRID: AB_2782993
goat anti-Chicken AlexaFluor 488	Abcam, Cambridge, UK	Cat#ab150173; RRID: AB_2827653
Bacterial and virus strains		
AAV9.Syn.GCaMP6s.WPRE.SV40	N/A	100843
AAV8-Syn-hM3D-Gq-mCherry	N/A	44361
AAV8-hSyn-hM4D-Gi-mCherry	N/A	44362
AAV8-hSyn-mCherry	N/A	114472
AAV1-flex-taCasp3-TEVp(Caspase)	N/A	44580
AAV8-hsyn-DIO-GFP	N/A	50457
AAV2-dio-EF1a-ChR2(H/R)-eYFP-WPRE-HGHpA	N/A	20298
Chemicals, peptides, and recombinant proteins		
Clozapine N-oxide	Sigma-Merck	C0832
Experimental models: Organisms/strains		
Long-Evans TH-cre rats	Rat Resource & Research Center, USA	RRRC#: 00659
Software and algorithms		
Prism	GraphPad	N/A
Med-PC	Med Associates	N/A
Synapse	Tucker Davis Technologies	N/A

RESOURCE AVAILABILITY

Lead contact

Further information and requests for resources and reagents should be directed to and will be fulfilled by the lead contact, John Apergis-Schoute (j.apergis-schoute@qmul.ac.uk)

Materials availability

This study did not generate new unique reagents.

Data and code availability

Any additional information required to reanalyze the data reported in this paper is available from the lead contact upon request.

EXPERIMENTAL MODEL AND STUDY PARTICIPANT DETAILS

All male Long-Evans TH-Cre rats (450 g-650 g) that were used in this study were housed in pairs in individually ventilated cages under temperature-controlled conditions (21°C ± 2°C; 40%–50% humidity) and kept under 12 hr light/dark cycle, with lights on at 07:00. Post-surgery, rats were housed with bedding materials recommended by the NC3Rs and never single housed. Water was available ad libitum and rats were food restricted maintaining their body weights at 85 ∼ 90% of their ad libitum fed body weights throughout the experiments.

All procedures were carried out under the appropriate UK government Home Office license authority (PPL number: PFACC16E2) in accordance with the Animals [Scientific Procedures] Act (1986).

METHOD DETAILS

Virus injection and implant surgery

Rats were deeply anesthetized using isoflurane (5% / 2 L/min for induction, 2% for maintenance). The head was shaved and pre-operative analgesia was administered (bupivacaine 150 μl at incision site and meloxicam 1 mg/kg sub-cutaneous). Rats were mounted in a stereotaxic frame (David Kopf Instruments) and a thermostatic blanket was used to maintain a stable body temperature throughout surgery (37–38°C). Constant monitoring of oxygen saturation and heart rate was performed with a pulse oximeter. A scalp incision was made and a hole was drilled above the A13 for virus injection and fiber implantation (A13 from Bregma AP -2.5; ML ±1.3; DV -7.4). In addition, holes were drilled anterior and posterior to attach four anchor screws. A virus injection needle (10 μl Hamilton Syringe) was lowered into the A13 (DV −7.4 mm, from dura) and 1 μl of virus was injected over 10 min using a syringe pump (11 Elite, Harvard Apparatus, CA). A fiber optic cannula was implanted at DV −7.3 mm (0.1 mm above the virus injection site) (ThorLabs CFM14L10, 400 μm, 0.39 NA, 10 mm, sterilised using ethylene oxide). A layer of radio-opaque dental cement was used to seal screws and cannula in place (C&B Super-Bond, Prestige Dental) and a headcap was formed using dental acrylic (DuraLay, Reliance Dental). Care was taken to leave approximately 5 mm of the ferrule protruding for coupling to optical patch cable for later photometry recordings. Rats were housed in pairs immediately following surgery and at least 3-4 weeks was allowed post-surgery for virus expression before testing began.

Cre-dependent viruses were injected bilaterally into the A13 (AP -2.5; ML ±1.3; DV -7.4). For fiber photometry experiments, 1 μl of undiluted virus expressing GCaMP6s (AAV9.Syn.GCaMP6s.WPRE.SV40, ∼1.9 × 10^{13} GC/ml; Addgene # 100843) was injected (0.1 μl /min) unilaterally in the A13 while for DREADD experiments viruses for reversibly activating (AAV8-Syn-hM3D-Gq-mCherry; Addgene # 44361), inhibiting (AAV8-hSyn-hM4D-Gi-mCherry; Addgene # 44362) or used as a control (AAV8-hSyn-mCherry; Addgene # 114472) were injected bilalterally. Similarly for caspase A13-DA ablation, AAV1-flex-taCasp3-TEVp(Caspase); (Addgene # 44580) or a control virus AAV8-hsyn-DIO-GFP (Addgene # 50457) was injected bilaterally. For anterograde and retrograde tracing experiments, 1 μl of the cre-dependent virus expressing ChR2 linked to eYFP (AAV2-dio-EF1a-ChR2(H/R)-eYFP-WPRE-HGHpA; Addgene # 20298) was injected (0.1 μl /min) bilaterally into the A13 and SC (AP -6.8; ML ±1.6; DV -2.4) or the RF (AP -10.1; ML ± 1.5; DV -8.8), respectively.

Fiber photometry

Fiber photometry equipment consisted of two fiber coupled light sources powered by LED drivers. A blue 470 nm LED (Thorlabs, M470F3) and violet 405 nm LED (Thorlabs, M405F1) were sinusoidally modulated at 211 and 539 Hz, respectively, and passed through filters (470 and 405 nm). Both light paths were directed, via dichroic mirrors positioned inside filter cubes (FMC4_AE(405)_E(460–490)_F(500–550)_S, Doric Lenses), through a fiber optic patch cord (MFP_400/460/LWMJ-0.48_3.5m_FCM_MF2.5, Doric Lenses). The patch cord was then mated, using a ceramic sleeve, to the implanted fiber optic cannula. Emitted fluorescence was collected via the same fiber, through the patch cord and focused onto a photoreceiver (#2151, Newport). A signal processor (RZ5P; Tucker Davis Technologies) and Synapse software (Tucker Davis Technologies) were used to control LEDs, to acquire the lowpass filtered signal (3 Hz), and to perform on-line demodulation of the signal. Demodulation of the two light sources allowed dissociation of calcium-dependent GCaMP6s signals (470 nm) and calcium-independent changes resulting from autofluorescence and motion artifacts (isosbestic 405 nm wavelength). All signals were acquired using Synapse Essentials software (Tucker Davis Technologies). Signals were sampled at 6.1 kHz (before demodulation) and 1017 Hz (after demodulation). Behavioral events (e.g., lever, presses, licks and sipper presentations) were time stamped by registering TTLs generated by the Med-PC system. Reaching and pasta handling events were aligned to paw-pellet/pasta contact by replaying videos of each session and manually adding time-stamps using Open Explorer software (Tucker Davis Technologies). The demodulated signals were filtered by using FFT to convert each signal from the time domain into the frequency domain, subtracting the 405 nm signal from the 470 nm signal, and then converting back into the time domain.[93] This corrected signal was used for all further analyses.

Histology

Immunohistochemistry was used to verify fiber implant sites in the A13 and to check the extent of regional viral expression. At the end of experiment, all rats were terminally anesthetized with isofluorane and sodium pentobarbital (5 ml/kg) before being transcardially perfused with ice-cold phosphate-buffered saline (PBS) followed by 4% paraformaldehyde (PFA). Following perfusion, brains were removed and placed in 4% PFA for 24 hr before being transferred to a cryoprotectant 30% sucrose solution in PBS for at least 3 days. 40 μm coronal sections were made using a freezing microtome and stored in 5% sucrose solution in PBS with 0.02% sodium azide until staining.

Free-floating sections were first incubated in blocking solution (3% normal goat serum, 3% normal donkey serum, 3% Triton-X in PBS) for 1 hr before incubation with primary antibodies (mouse anti-tyrosine hydroxylase 1:1000, AB152 (Merck Millipore; rabbit anti-mCherry 1:1000, ab167453; chicken anti-GFP 1:1000, ab13970; Abcam, Cambridge, UK) in blocking solution at room temperature on a shaker for 18 hr. Next, sections were incubated with secondary antibodies with either donkey anti-mouse AlexaFluor 488 (1:1000), donkey anti-Rabbit 594 (1:1000) or goat anti-Chicken AlexaFluor 488 (1:1000), (Abcam, Cambridge, UK) in PBS for 120 min at room temperature. Sections were mounted on slides using Vector Shield hard-set mountant (Vector Labs, UK). Between

steps, sections were washed three times with PBS for 5 min and gently agitated on a laboratory shaker. Slices were imaged using an epifluorescent microscope (Leica, UK) to determine fiber placement and virus expression with the Paxinos and Watson (2007) rat brain atlas used as reference.

Behavioral Paradigms

Lever pressing, chain-pulling and two-bottle choice experiments took place in operant behavior chambers (Med Associates, VT, USA; 25 cm × 32 cm × 25.5 cm) housed inside large sound attenuating chambers. All behavioral experiments were video recorded using a Logitech C920 webcam. The lever, the sipper and the cue light were located on the same wall within the chamber. For tests reinforced with a liquid reward, a grid floor, comprised of stainless steel rods, was used in conjunction with contact lickometers, to record individual licks as rats consumed solutions from a spout recessed 5–10 mm from the chamber wall. For tests reinforced with sugar pellets, one pellet was delivered into a food hopper for each successful response. In these tasks a light signalled the beginning of an active trial. For tests reinforced with a liquid reward, sippers were extended after successful responses and were made available for 5 sec when lick contact was made. If there was no contact sippers were retracted after 20 sec. For DREADD experiments, saline or clozapine N-oxide (CNO) at 1 mg/kg was injected 45 min before the start of experiments. When multiple tests were conducted, those tests were run on different days, so that there was no more than 1 behavioral test per day per injection of CNO.

To allow for sufficient viral expression all training was started at a minimum 3 weeks after surgery and carried on until animals reached behavioral criteria which for lever-press, chain-pull or sipper choice trials was 20 successful trials. For the reaching task, rats were required to successfully retrieve 80% of pellets offered. In the 2-bottle choice task criteria was reached within a single session while that for lever pressing and chain-pulling was reached in approximately four to five 1-hour sessions. The same photometry animals were used in multiple paradigms (Sequence: 2-bottle choice, FR1, FR3, CP, reaching and pasta handling tasks). Two additional animals were used in the lever pressing and 2-bottle tasks. To minimize over-training effects, the analysed photometry signals were recorded in the session immediately after animals reached criteria.

For the 2-bottle choice, LP1, LP3 and CP tasks each session was terminated after 20 trials regardless of successful responses. Each trial was separated by a mean intertrial interval (ITI) of 20 sec (min 10; max 30) and if no responses were made then the lever/sippers remained available for 30 s. However, once a lever was pressed or lick was made, the lever/sippers remained extended for 5 sec before retraction. Coincident with sipper activation, the cue light located above the sipper hole was turned on and remained on until the lever/sipper was retracted. Sippers took ~2 sec from activation until the rat could reach them to drink.

Lever pressing task

Using a FR of reinforcement rats were trained to press 1, 3 or 5 times for a reward (sipper access or sucrose pellet). In the Progressive Ratio, increasing number of operant responses are needed for each successive reward (5, 10, 15, etc). A 5 sec delay was imposed between the operant response and reward availability.

Two-Bottle Free Choice Task

Prior to testing, rats were habituated to the presence of two drinking bottles and solutions for 3 days in their home cage. Following this acclimation, two different experiments were performed where rats were given simultaneous intermittent access to two sippers each containing a different solution: either sucrose or water or sucrose and condensed milk (Carnation; 50% with water). The bottles were presented a total of 20 times each and bottle position was always counterbalanced and to encourage choice behavior the position of each bottle was switched between training and testing sessions. In all trials, the light cue was present at the same time as the sippers were extended. All training sessions used similar solutions as those used during testing.

Chain Pulling

The rat chain-pulling test was performed as described in detail elsewhere.[94] Instrumental procedures were performed using a metal chain 0.8 cm in diameter and 16 cm in length, which was attached to electronic switches mounted on the chamber ceiling. Following a successful pull, rats licked the available sipper while simultaneously gripping the chain and so behaviorally the motor response was largely inseparable from the sipper access.

Reaching task

A rodent skilled reaching task was used to evaluate forelimb motor function. The single pellet reaching box was rectangular, constructed of clear Plexiglas whose dimensions are 25x25 cm, and 50 cm high and designed to allow filming of the reaching behavior.[32] A vertical slot 10 mm wide and 10 cm high on one wall opened to an external shelf that was mounted 3 cm above the floor. Rodents were trained to reach out through a slot to grab and retrieve a sucrose pellet for them to consume. Commercial sucrose pellets weighing 45 mg were initially available on the cage floor and then within a tongue distance on the shelf to associate the cage and shelf position with a sucrose reward. Pellets were incrementally distanced on the shelf until the animals were forced to reach with a hand to retrieve the food. Food restricted rats were acclimated for 1 week by placing them in the reaching task box for 10 min each day.

On each trial a pellet was manually placed on a ledge in front of the opening. A new trial began after animals retracted from the task (i.e. both paws were on the floor and/or rat was away from the opening) and a pellet was placed on the ledge. The ITI was approximately on average 60 sec and sessions lasted until 80% of pellets (30-35 pellets) were successfully retrieved. The pellet was always placed on the same indentation off-centrally to the opening to prevent rats from lapping the food with their tongue. Successful reaches were considered when sucrose pellets were reached for, grasped and consumed and failures were when sucrose pellets were never properly grasped and eaten.

Pasta test

The pasta test used was based on Tennant et al.[34] Uncooked Skinner brand vermicelli pasta (1.5 mm diameter) were cut to 7 cm lengths using a razor blade. To overcome neophobic responses and to establish skill in handling, animals were homecage exposed to the pasta pieces between 5-10 days of exposure, 4 pieces each time, prior to testing. Rats were also similarly habituated to pasta in the testing chamber (3-5 sessions, 25x25 cm, and 50 cm Plexi-glass chamber). On a test day, rats were placed into the testing chamber and were given one 7 cm piece of vermicelli at a time by an experimenter. Once rats had finished consuming this piece there was a 1 min inter-trial interval before they were given a new piece. Total session time was 1 hr.

Grip Strength

This test is based on the tendency of a rat to instinctively grasp a bar or a grid when suspended by the body and permits assessment of forelimb strength. The test apparatus (Grip Strength Meter, Ugo Basile, Italy) consisted of a grasping bar attached to a force transducer in order to measure the maximum force applied by the rat during the pull. The unit of force used is grams-of-force. Each animal was handled via the body and brought near the bar, allowing the grasping of the grid with both forepaws and then gently pulled back until they released it. Measurements were discarded when rats only used one paw, used its hind paws, turned backwards during the pull, or released the bar without resistance. Animals were trained and tested on two consecutive days, using the same protocol. Five such measurements were obtained for each animal, and the resting period between each pull was 1 min.[95] The three best of each session were averaged and used for analysis. Results were expressed as total force (gm) and as normalized by body weight (force in grams/body weight in grams).

Locomotion & Exploration

Rats were tested in a brightly illuminated open arena made of opaque white Plexiglass (50 × 50 cm floor area). Each animal was placed gently on the central zone and its behaviors were recorded by a camera for 15 min. The neurobehavioral parameters were computed offline at a rate of 30 frames/s using a video-tracking software (ANY-maze, Stoelting, CO, USA). Briefly, total distance traveled and time spent in the center and bordering regions was quantified by automated video-tracking and the percentage of time spent in the center of the arena was calculated. Tests were conducted between 10:00 and 15:00h. In order to maintain arena novelty, each rat was tested with a frequency of once a week and the context was adjusted by adding local and distal cues (i.e. striped walls).

QUANTIFICATION AND STATISTICAL ANALYSIS

Photometry analysis was conducted using Python running in a custom Jupyter Notebook. TDT files including both photometry signals and event time stamps were loaded using the tdt package. Photometry signals were corrected using the isosbestic signal as a reference as described earlier in the STAR Methods and this corrected signal was used for all further analysis. Peri-event photometry signals were extracted around an event of interest (e.g. lever press) and normalised by z-scoring on a trial-by-trial basis using a baseline epoch as reference. For lever pressing and chain pull tasks, we used a 3 second analysis epoch centered on the event of interest (e.g. 1.5 sec before and 1.5 sec after operant response) and the baseline epoch was a 3 sec period immediately preceding this analysis epoch. For licking behavior in 2-bottle choice task, the analysis epoch was the 5 sec after start of licking during which the sipper was available and baseline epoch was 5 sec preceding this epoch. For reaching task, the analysis epoch was a 3 sec epoch corresponding to the first contact with the pellet and the baseline epoch was a 3 sec epoch between -5 and -2 sec before this contact. For the pasta handling task, the analysis epoch was a 5 sec epoch following the first contact with the pasta and the baseline epoch was a 5 sec epoch immediately preceding this contact. These values were imported into Prism to conduct statistical analyses. All data were expressed as means and standard error of means (SEM). Alpha was set at $P < .05$, all significance tests were two-tailed, and Sidak or Tukey's HSD was used to correct for multiple comparisons.